GRATING-ENHANCED COHERENT IMAGING

Jeffrey P. Wilde[1], *Joseph W. Goodman*[1], *Yonina C. Eldar*[1,2], *Yuzuru Takashima*[1]

[1]Department of Electrical Engineering,Stanford University, Stanford, CA
[2]Department of Electrical Engineering,
Technion, Haifa 32000, Israel
Email: jpwilde@stanford.edu

ABSTRACT

We describe a coherent imaging technique that utilizes a diffraction grating placed near the object to alias high spatial frequency information through the imaging system pupil. The resulting optical field in the image plane is detected by means of digital holography. Multiple measurements are taken with the grating shifted by a fraction of its period between exposures. Linear signal processing is then used to separate the aliased spectral components, and Fourier techniques are applied to reconstruct high-resolution images. Experimental results validate the approach, yielding an enhancement in resolution by a factor of 2.6 when using five diffracted beams (orders up to ±2).

Keywords — Superresolution, Image reconstruction techniques, Synthetic-Aperture Microscopy

1. INTRODUCTION

A variety of synthetic aperture approaches have been previously investigated to provide improved resolution of linear imaging systems beyond the intrinsic cutoff frequency as defined by the numerical aperture (NA) and wavelength (but still constrained by the far-field resolution limit of $\lambda/2$, excluding techniques based on a nonlinear spatial response of the object to the illumination light). Doing so allows one to use a low-NA objective lens having a long working distance and large field-of-view, while simultaneously obtaining resolution comparable to a higher-NA system.

One superresolution technique, first reported in 1966, involves the use of two static gratings [1,2], one near the object and the other near the image plane, but this leads to ghost image formation that significantly restricts the field of view. Alternatively, the two gratings can be synchronously moved, and the detected image temporally averaged in order to eliminate the spurious ghost images [3,4], but this configuration is more complicated to implement and has only been demonstrated with unity magnification. Additional techniques include structured illumination of fluorescent objects [5,6], as well as various oblique illumination schemes [7,8] in which the range of illumination angles is restricted by the NA of the illumination optics or by the source configuration as in the case of a VCSEL array [8].

We present here a coherent imaging approach based on the use of a single grating placed before or after the object in order to alias high-frequency content through the pupil. Our approach is based on the recently proposed modulated-wideband converter (MWC), that was designed to reduce sampling rate in analog-to-digital conversion [9,10]. The MWC allows recovery of signals from the output of several lowpassed versions of the signal, where the different branches correspond to modulations of the input by a periodic function. Here we propose an optical implementation of the MWC in which the lowpass filter is replaced by a low NA lens, and the modulations are replaced by an appropriate grating.

The grating produces copies of the object's angular spectrum that are shifted from one another by multiples of the grating frequency. This set of spectra is low-pass filtered by the pupil. Within the pupil, the various shifted portions of the object spectrum combine linearly with coefficients ideally given by the Fourier series coefficients of the grating. Digital holography is employed to detect the complex amplitude of the optical field in the image plane. Multiple measurements are taken with the grating shifted by a fraction of its period between exposures. Linear signal processing, similar to that used for structured illumination and for the MWC, is then used to de-alias the spectral components and reconstruct a high-resolution image, providing both intensity and phase distributions.

The primary benefit of this new approach centers on the fact that it is a rather simple method, based on a single grating element, for generating a wide synthetic aperture. It can yield large plane-wave illumination angles without the need for high-NA illumination lenses. Additionally, this grating-enhanced technique yields quantitative phase information and can be used with non-fluorescent objects.

2. THEORETICAL FORMULATION

In this section, we limit the analysis to a 1-D formulation, but the extension to 2D is straightforward. Consider a coherent imaging system and suppose that a high-frequency grating is placed in close proximity to the object being

imaged, either just before the object or just after it. The grating amplitude transmittance is a periodic function with period $1/f_g$, which we represent by $P(x)$ and can be expanded in a complex Fourier series:

$$P(x) = \sum_{n=-\infty}^{\infty} p_n \exp\left(-j2\pi n f_g x\right) \quad (1)$$

Furthermore, we assume that the grating has been fabricated such that it possesses a finite set of lower-order Fourier coefficients p_n that are approximately equal in magnitude, meaning that all the plane wave components illuminating the object are of approximately equal magnitude, while all the other higher-order p_n are close to zero. For example, a Dammann phase grating provides such a response.

If $t_0(x)$ represents the complex amplitude transmittance of the object, which is the quantity we wish to recover, the field leaving the sandwiched object and grating is given by

$$t_o(x)P(x) = t_o(x)\sum_{n=-\infty}^{\infty} p_n \exp\left(-j2\pi n f_g x\right). \quad (2)$$

The spectrum of $t_0(x)P(x)$, which is incident on the pupil plane, is then given by

$$U(\nu) = T_o(\nu) \otimes \sum_{n=-\infty}^{\infty} p_n \delta(\nu - n f_g), \quad (3)$$

where $T_o(\nu)$ is the object spectrum and $\otimes$ signifies convolution. We explicitly assume that the grating is located before or in contact with the object. If the grating follows the object, then only the propagating portion of the object spectrum for normal incidence should be considered.

In the absence of the grating, the finite pupil of the system will restrict the light that passes through the pupil stop to a finite region of the spectrum. Consequently, important information about the object detail is lost. The effect of the grating is to multiplex many different parts of the object spectrum into the pupil. The resulting image will not resemble the object, but with a series of images (N images to expand the spectrum by a factor $\le N$), each taken with an appropriate change in the grating Fourier coefficients p_n, it is possible to unscramble the overlapping regions of the spectrum and stitch them back together in proper order, yielding a much broader spectrum of the object than would otherwise pass the pupil. One possible set of changes of the spectral coefficients p_n can be obtained by translating the grating between image captures by a fraction of the period, in particular by $1/f_gN$. Each such translation changes the phase of the n^{th} grating Fourier component by $\Delta\phi_n = 2\pi n / N$. This follows the approach in [9,10] for generating multiple modulations in the MWC.

In order to accomplish this extension of resolution, it is necessary to measure the *complex amplitude* of the field in the image plane. This can be done via digital holography by bringing in a tilted reference wave, coherent with respect to the field in the image plane, to interfere with this field and thus create a hologram. The complex field in the image plane can then be recovered by digitally filtering the hologram to eliminate all but one sideband, and translating that side band to be centered on zero frequency.

We now briefly consider the digital processing performed on a set of $2N+1$ measured fields in the pupil (we use $2N+1$ measurements rather than N measurements for mathematical convenience, and attempt to expand the spectrum by a factor $\le 2N+1$). Using a one-dimensional analysis, the k^{th} detected image amplitude can be written as

$$A_k(\nu) = \sum_{n=-N}^{N} p_{k,n} T_o(\nu - n f_g)\,\mathrm{rect}(\nu / 2 f_p), \qquad k = -N, \ldots N \quad (4)$$

where the grating coefficients $p_{k,n}$ change for each of the $2N+1$ image captures, the rectangle function represents the finite pupil having a half-width frequency of f_p, and we have assumed that the grating frequency is chosen such that $f_g = \sigma f_p$, where σ is an obliquity factor between 0 and 1. In this way, the ± 1 diffraction components reside within the pupil, and the grating therefore produces aliasing with overlapping spectral regions. In practice, σ is taken to be between 0.80-0.95. We utilize the spectral overlap regions in signal processing, but this overlap is also needed when extending to 2D with a circular pupil so that complete coverage of the broadened spectral domain is obtained without gaps.

Equation 5 can be rewritten in matrix-vector form as

$$\vec{A}(\nu) = P\vec{T}(\nu) \quad (5)$$

where

$$\vec{A}(\nu) = \begin{bmatrix} A_{-N}(\nu) \\ \vdots \\ A_N(\nu) \end{bmatrix}, \quad (6)$$

$$\vec{T}(\nu) = \begin{bmatrix} T_o(\nu + N f_g)\,\mathrm{rect}(\nu / 2 f_p) \\ \vdots \\ T_o(\nu - N f_g)\,\mathrm{rect}(\nu / 2 f_p) \end{bmatrix}, \quad (7)$$

and P is a $(2N+1)$ x $(2N+1)$ matrix

$$P = \begin{bmatrix} p_{-N,-N} & \cdots & p_{-N,N} \\ \vdots & \vdots & \vdots \\ p_{N,-N} & \cdots & p_{N,N} \end{bmatrix}. \quad (8)$$

Now if the grating constants are chosen such that the matrix P is non-singular and well conditioned, then P^{-1} exists and the spectral segments can be separated through

$$\vec{T}(\nu) = P^{-1}\vec{A}(\nu). \quad (9)$$

Once the individual spectral segments are known, they can be translated to their proper frequency positions in order to synthesize a broader spectrum. Specifically, the image spectrum half-width increases from f_p to $(\sigma N+1)f_p$, where $(\sigma N+1)$ is the resolution gain factor.

During signal post processing, we make use of the overlap between adjacent segments to help compute the complex amplitudes for grating orders beyond the first order, which takes into account potential relative phase shifts that can occur during propagation to the image plane. In this way a self-consistent stitching together of the spectral segments is created. More than $2N+1$ measurements can be made as a form of oversampling, with the result that the P matrix is no longer square but can still be readily inverted through use of the psuedoinverse. Lastly, because the imaging system is coherent, no OTF compensation is required, unlike the case of incoherent imaging with structured illumination [11].

3. DATA ANALYSIS

The ideal square P matrix, based on a set of equal-increment grating steps, takes on a simple form with matrix elements given by $exp[-j2\pi nm/(2N+1)]$ where n is a row index (0 to $2N$) and m is a column index ($-N$ to N). This matrix is unitary with an inverse equal to its conjugate transpose. In practice, there are errors in the grating positioning as well as a small phase drift of the interferometer in between exposures. Also, the imaging system may be slightly misaligned so as to impart different average wavefront error to otherwise symmetric diffraction orders. All of these effects conspire to perturb the P matrix from its ideal form.

However, these perturbations can be accommodated by employing a two-pronged approach. First, assume that the center of the signal spectrum is much larger than the wings. In this case, the complex amplitudes of the 0 and ±1 order beams, which pass through the pupil, can be estimated by directly measuring the corresponding spectral peaks [12]. Note that because the imaging system is coherent, the ±1 peaks are not attenuated by the transfer function, making this technique even more attractive compared to the incoherent case. Next, we consider the ±2 order beams. For these diffracted components the coefficients cannot be directly measured in the same way, but they can instead be estimated by finding values that minimize the sum of the squared difference across pixels in regions where the ±1 and ±2 spectral components overlap with one another. This approach can be extended to deal with higher orders.

4. EXPERIMENTAL RESULTS

An experimental test system with 1-D resolution enhancement, illustrated in Figure 1, has been constructed in order to demonstrate the technique. A He-Ne laser serves as a coherent source, and the beam is split to form a Mach-Zehnder interferometer with the imaging system placed in one arm. A low-cost CMOS camera is used for off-axis digital holographic detection. For simplicity, a Ronchi ruling is used as the grating in this initial work. Because such a grating has multiple diffraction orders with varying strengths, we implement front-end illumination optics to limit the number of transmitted orders and to balance their powers via spatial filtering. The underlying technique, though, will ultimately not rely on such illumination optics. The grating is moved by a piezo-electric actuator in a sequence of equal-increment steps across one period. At each step a digital hologram is captured. The sequence of holograms is post-processed as described in Sections 2 and 3 to yield a much broader image spectrum.

Using a Ronchi grating of 98.4 lp/mm (2500 lp/in) with an illumination system magnification of 1.25 yields an effective grating illumination frequency of 78.7 lp/mm. A variable aperture iris is adjusted to set to the coherent imaging passband cutoff frequency to approximately 100 lp/mm ($NA_0 = 0.063$). In this way the ±1 orders are able to pass through the imaging system ($\sigma = 0.79$), but higher orders are cut off. A spatial filter mask in the illumination path restricts the highest orders to ±2 and also approximately equalizes the powers of the diffracted beams.

The object is a standard USAF test target (Group 7, Elements 4-7). Five hologram exposures are recorded while stepping the grating in five equal-increment steps (2.03 μm/step). Digital post processing yields the five separate spectral regions. Figure 2 shows the results when the center three regions (0, ±1 orders) are combined, and Figure 3b is the corresponding image with horizontally enhanced resolution. The resolution gain factor is 1.8 (i.e., $NA_1 = 0.11$). The observed new cutoff frequency of 181 lp/mm (Group 7, Element 4) agrees very well with the expected theoretical value of $NA_1/\lambda = 180$ lp/mm. Similarly, Figure 4 shows the extended spectrum using all five components. In this case the resolution gain factor is 2.6 ($NA_2 = 0.16$), and the corresponding enhanced image in Fig. 5b shows the smallest feature set on the test target (228 lp/mm; Group 7, Element 6) to be well within the new cutoff of 259 lp/mm.

5. CONCLUSIONS

We describe a fairly straightforward approach for extending the resolution of a coherent optical imaging system by applying the principles behind the recently proposed MWC. Our approach consists of placing a grating near the object and shifting it in a sequence of equal-increment steps. Coherent detection via digital holography allows linear signal processing to be used to de-alias the transmitted spectrum and reconstruct images with a demonstrated resolution gain of 2.6. Higher gains, in the range of 4-5, should be possible by using a Dammann grating with more orders. 2-D enhancement can be obtained by rotating the grating and repeating the measurements.

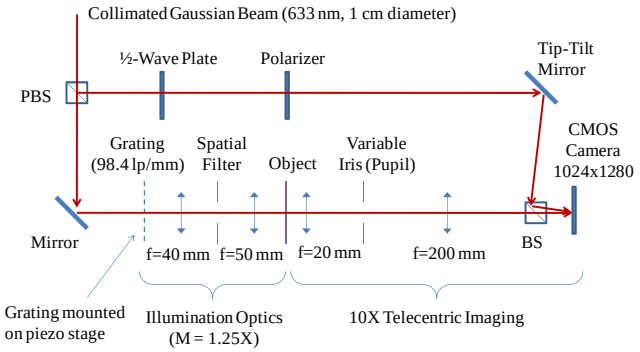

Figure 1. Experimental setup.

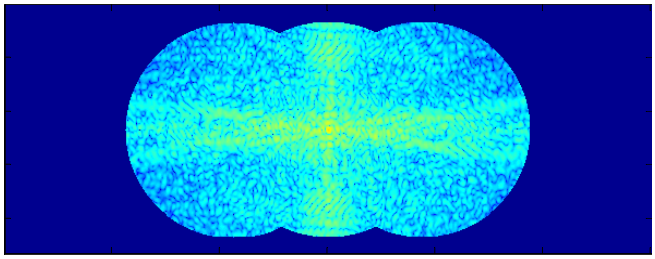

Figure 2. Reconstruted image spectrum magnitude using three diffracted beams (0 and ±1 orders).

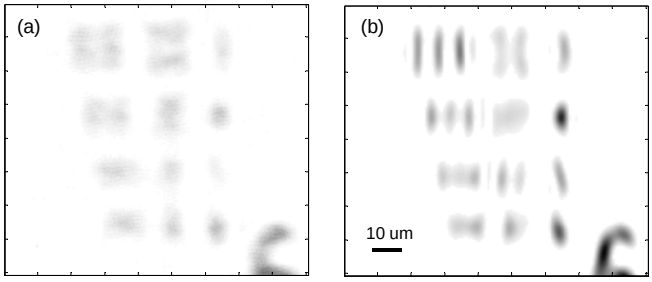

Figure 3. Test target images: (a) conventional image formed by NA_0 = 0.065 system, (b) higher resolution image (NA_1 = 0.12; horizontal direction) formed by an inverse Fourier transform of the spectrum in Figure 2 .

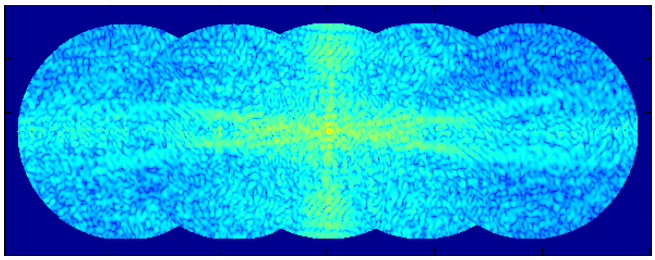

Figure 4. Reconstruted image spectrum magnitude using five diffracted beams (0, ±1 and ±2 orders).

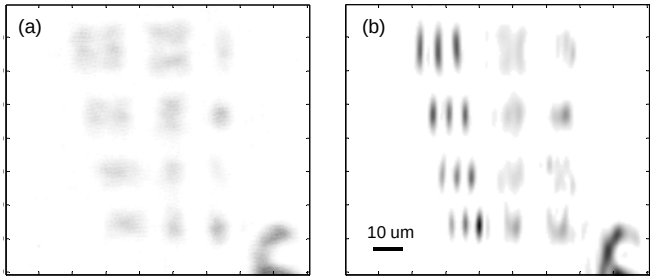

Figure 5. Test target images: (a) conventional image formed by NA_0 = 0.065 system, (b) higher resolution image (NA_2 = 0.16; horizontal direction) formed by an inverse Fourier transform of the spectrum in Figure 4.

6. REFERENCES

[1] W. Lukosz, "Optical systems with resolving power exceeding the classical limit," JOSA **56,** 1463-1472 (1966).

[2] J. Garcia, V. Mico, D. Cojoc and Z. Zalevsky, "Full field of view super-resolution imaging based on two static gratings and white light illumination," Appl. Opt. **47**, 3080-87 (2008).

[3] W. Lukosz, "Optical systems with resolving power exceeding the classical limit. II," JOSA **57,** 932-941 (1967).

[4] D. Mendlovic, I. Kiryuschev, Z. Zalevsky, A. W. Lohmann and D. Farkas, "Two-dimensional superresolution optical system for temporally restricted objects," Appl. Opt. **36**, 6687-6691 (1997).

[5] M. G. L. Gustafsson, "Nonlinear structured-illumination microscopy: Wide-field fluorescence imaging with theoretically unlimited resolution," PNAS **102**, 13081-13086 (2005).

[6] A. Neumann, Y. Kuznetsova and S. R. J. Brueck, "Structured illumination for the extension of imaging interferometric microscopy," Opt. Exp. **16**, 6785-6793 (2008).

[7] A. Faridian, D. Hopp, G. Pedrini, U. Eigenthaler, M. Hirscher and W. Osten, "Nanoscale imaging using deep ultraviolet digital holographic microscopy," Opt. Exp. **18**, 14159-14164 (2010).

[8] V. Mico, Z. Zalevsky, P. Garcia-Martinez and J. Garcia, "Superresolved imaging in digital holography by superposition of tilted wavefronts," Appl. Opt. **45**, 822-828 (2006).

[9] M. Mishali and Y. C. Eldar, "From theory to practice: sub-Nyquist sampling of sparse wideband analog signals," IEEE Journal of Selected Topics on Signal Processing **4**, 375-391 (2010).

[10] M. Mishali, Y. C. Eldar, O. Dounaevsky and E. Shoshan, "Xampling: Analog to digital at sub-Nyquist rates," IET Circuits, Devices & Systems **5,** 8–20 (2011)

[11] S. A. Shroff, J. R. Fienup and D. R. Williams, "OTF compensation in structured illumination superresolution images," Proc. SPIE **7094**, 709402 (2008).

[12] S. A. Shroff, J. R. Fienup and D. R. Williams, "Phase-shift estimation in sinusoidally illuminated images for lateral superresolution," JOSA A **26**, 413-424 (2009).